In Situ Measurement of Dissolved Hydrogen during the Liquid-Phase Hydrogenation of DinitrilesMethod and Case Study

ARTICLE *in* INDUSTRIAL & ENGINEERING CHEMISTRY RESEARCH · OCTOBER 2005

Impact Factor: 2.59 · DOI: 10.1021/ie050612y

4 AUTHORS, INCLUDING:

Peter Schärringer
Technische Universität München
7 PUBLICATIONS **69** CITATIONS
SEE PROFILE

Thomas Ernst Müller
RWTH Aachen University
124 PUBLICATIONS **4,255** CITATIONS
SEE PROFILE

Johannes A Lercher
Technische Universität München
544 PUBLICATIONS **11,864** CITATIONS
SEE PROFILE

In Situ Measurement of Dissolved Hydrogen during the Liquid-Phase Hydrogenation of Dinitriles—Method and Case Study

Peter Schärringer, Thomas E. Müller,* Wolfgang Kaltner, and Johannes A. Lercher

Technische Universität München, Department Chemie, Lichtenbergstrasse 4, 85747 Garching, Germany

Despite the importance of gas/liquid/solid multiphase systems in the production of chemicals on an industrial scale, measuring the concentration of gases dissolved in the liquid phase—a prerequisite for determining basic reaction data such as rate and adsorption constants—remains challenging. Recently, a new permeation probe became available, which allows in situ measurement of gas concentrations in liquids. To evaluate potential applications, the probe was used to follow the concentration of dissolved hydrogen during the cobalt-catalyzed reduction of an aliphatic dinitrile to the corresponding diamine. The changes in the hydrogen saturation level during the reaction were compared to the gas−liquid (G−L) mass transfer characteristics of the reactor as determined by k_La measurements. Under the reaction conditions used, G−L mass transfer became the rate-determining step when the stirring speed was decreased. The permeation probe allowed for evaluating the significance of G−L mass transfer in a straightforward manner.

1. Introduction

Frequently, a solid catalyst is used to accelerate the reaction between a gaseous reactant and a liquid or dissolved substrate. Examples are manifold and include hydrogenation reactions. Mathematical models of such three-phase gas/liquid/solid systems (G−L−S) are often based on kinetic data obtained in laboratory-scale slurry reactors. However, to derive valid data, special attention has to be given to mass transport limitations. During hydrogenation, molecular hydrogen has to diffuse from the gas into the liquid phase, across the stagnant layer around the catalyst particles, and into the catalyst pores before adsorbing at the catalytically active centers (Figure 1). If slow relative to the rate of reaction, the transport steps can lead to a significant reduction in the rate of the overall process. Both the performance of a catalyst and the mechanistic details can be evaluated properly only when the observed rate of reaction is determined by the chemical reaction at the active site. Therefore, it is an essential prerequisite for the establishment of an intrinsic kinetic model to verify the absence of transport effects.[1] However, additional experiments [2] are necessary to rule out mass transfer limitations. During catalyst screening, for example, the absence of mass transfer limitations has to be confirmed for every single catalyst when significant activity differences are observed.

Recently, a new permeation probe for in situ measurement of the partial pressure of dissolved gases has become commercially available.[3] Provided the Henry coefficient has been determined, the concentration of dissolved gases can be measured with this probe, even when the vapor pressures of the single components in the reaction mixture are unknown. Therefore, the probe might provide a useful tool for evaluating the extent of G−L mass transfer limitations in the overall reaction sequence (see Figure 1). In this study, the permeation probe was used to measure the concentration of dissolved hydrogen during a typical hydrogenation reaction in a laboratory-scale slurry reactor. So far, the use of this permeation probe for in situ measurements had not been reported. The results were related to classic methods for the identification of mass transfer limitations to unambiguously establish the working regime.

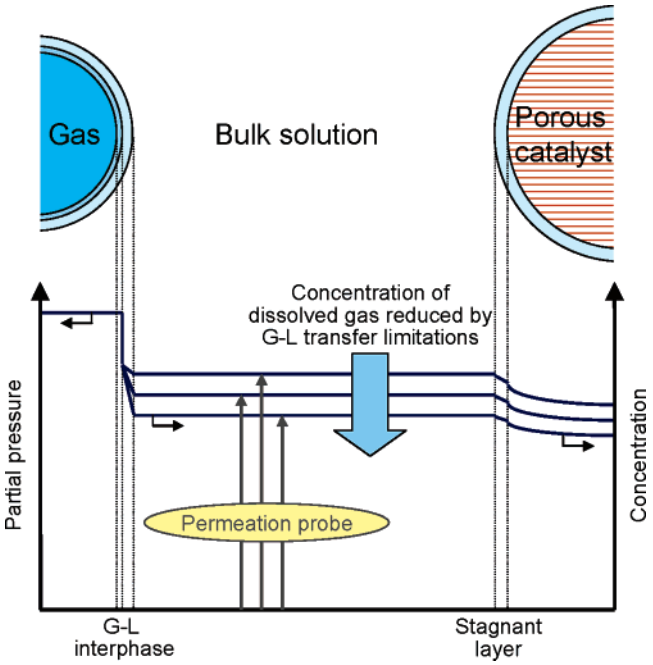

Figure 1. Possible concentration profile for gas/liquid/solid multiphase systems in the presence of mass transport limitations, illustrating the importance of measuring the gas concentration in bulk solution.

2. Experimental Section

2.1. Materials. A commercially available silica-supported cobalt catalyst was used as received without further activation. Three different particle sizes (<100, 100−200, and 200−300 μm) were available. Liquid

* To whom correspondence should be addressed. Fax: +49-89-28913544. E-mail: thomas.mueller@tum.de.

10.1021/ie050612y CCC: $30.25
Published on Web 10/22/2005

ammonia and hydrogen were received from Messer Griesheim with 99.98% and 99.999% purity, respectively.

2.2. Catalytic Experiments. The hydrogenation of the dinitrile was performed in a tank reactor (160 mL, Parr Instruments) with a hollow shaft stirrer for gas entrainment. The reactor was operated in semibatch mode at constant pressure. The hydrogen consumption was recorded with a mass flow controller (Bronckhorst). In a typical experiment, the autoclave was charged under nitrogen atmosphere with a fresh catalyst sample (4 g with a particle diameter of $<100\ \mu$m). After adding liquid ammonia (75 mL), the reactor was pressurized with hydrogen to 2.0 MPa and heated to 363 K. The reactor was then charged with dinitrile (37 mL), the hydrogen pressure was adjusted to 3.0 MPa, and the stirrer was started (start of the reaction). Temperature, hydrogen pressure, hydrogen consumption, and hydrogen concentration in the carrier gas of the permeation probe were recorded during each experiment. Samples of the liquid phase were periodically withdrawn and analyzed with a Fisons GC 8160 gas chromatograph equipped with FID (flame ionization detection) detector and 30 m Optima 5 column.

2.3. Gas−Liquid Mass Transfer Coefficient k_La. The gas−liquid volumetric mass transfer coefficient k_La was determined with the pressure-step-method.[4] After charging the reactor with dinitrile (37 mL), the system was purged with nitrogen. Ammonia (75 mL) was added, and the liquid was stirred at the pressure P_0 and the temperature T (363 K) until equilibration. The stirrer was stopped, and the pressure in the reactor increased rapidly (within 1 s) to P_m. As soon as thermal equilibrium was reached (ca. 10 s), the stirrer was started and the pressure drop was recorded until the final pressure P_f was obtained. Integration of the mass balance between $t = 0$ ($P = P_m$) and t ($P = P(t)$) provides the following equation:

$$\ln\left(\frac{P_m - P_0}{(1+K)(P - P_0) - K(P_m - P_0)}\right) = \frac{1+K}{K}k_La t \quad (1)$$

with

$$K = \frac{P_f - P_0}{P_m - P_f} \quad (2)$$

The k_La value is calculated from the slope of a plot of the left side of eq 1 vs. time.

2.4. Measuring the Concentration of Dissolved Hydrogen with the Permeation Probe. The hydrogen concentration in the liquid phase was determined with a Fugatron HYD-200 dissolved hydrogen analyzer. A miniature permeation probe with a 7.8 mm outer diameter (MIN-100 Fugatron probe) and a standard permeation probe with an 18 mm outer diameter (STD-100 Fugatron probe) were available. One of the probes was mounted in the reactor flange using standard 1/8 in. tube fittings (Figure 2) and immersed into the liquid phase. The working principle of the instrument is based on the permeation method.[5] At the tip of the probe, the dissolved hydrogen permeates through a dense membrane of a fluorinated polymer with 200 μm thickness and 20 mm^2 and 8 cm^2 area (MIN-100 and STD-100 Fugatron probes, respectively). Internally, the probe is purged by a constant carrier gas stream of 1% O_2 in N_2 (10 mL·min^{-1}) and the concentration of permeated hydrogen molecules is analyzed. The concentration of hydrogen in the carrier gas is directly proportional to the partial pressure of hydrogen outside of the probe tip.

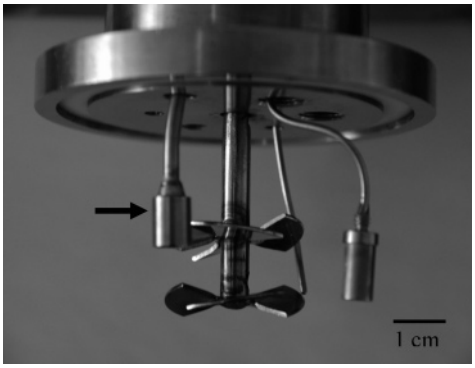

Figure 2. Miniature gas permeation probe MIN-100 (outer diameter 7.8 mm) implemented in the laboratory reactor.

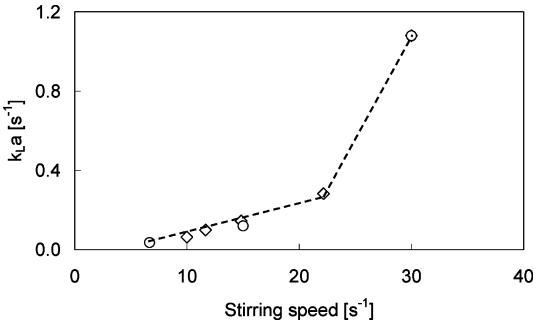

Figure 3. Gas−liquid mass transfer coefficient k_La in the laboratory reactor as a function of stirring speed: (◇) $T = 353$ K; (○) $T = 363$ K.

3. Results and Discussion

3.1. Gas−Liquid Mass Transfer. To determine the mass transfer characteristics of the autoclave used in this study, the G−L mass transfer coefficient k_La was measured for hydrogen at various stirring speeds and two temperatures (353 and 363 K) (Figure 3). The solvent mixture used in the k_La measurements had the same composition as the reaction mixture in the catalytic experiments (volume ratio of ammonia to dinitrile = 2:1). For both temperatures, the k_La value increased linearly with the stirring speed up to 22 s^{-1}. However, at a stirring speed of 30 s^{-1}, a considerably higher k_La value was found than would have been expected with a linear behavior over the whole range of stirring speeds. This can be attributed to the onset of gas insertion via the hollow shaft of the stirrer at a speed of about 24 s^{-1}. In the temperature range investigated, no significant temperature dependence of the k_La was observed. The k_La values obtained for the autoclave used in this study are similar to values reported for comparable reactors with gas-inducing stirrers.[6,7]

The permeation probe was used to assess the saturation level of the liquid phase with hydrogen. In preliminary tests,[8] the cross-sensitivity with solvent and reactants as well as the influence of liquid velocity were explored. No signal was observed when the permeation probe was immersed in ammonia and/or dinitrile without hydrogen being present. This shows that there was no cross-sensitivity with the reaction mixture. The velocity of the liquid at the probe was changed by varying the stirring speed. The signal increased by 6%

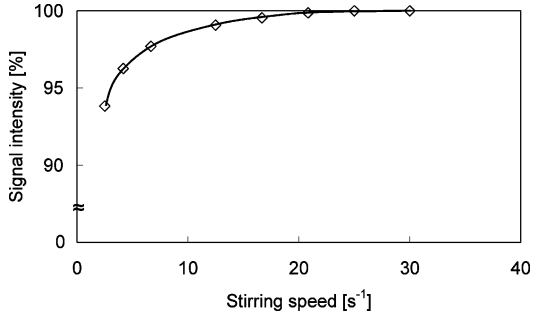

Figure 4. Relative signal intensity (MIN-100 probe) as a function of the stirring speed in a 2:1 mixture of ammonia and dinitrile at $T = 363$ K and a partial pressure of hydrogen of 3.0 MPa.

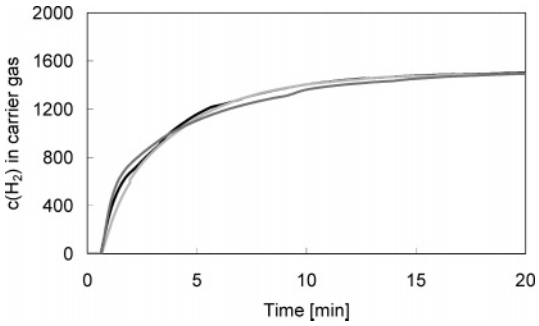

Figure 5. Response of the permeation probe (MIN-100) to a hydrogen pressure step (from 0 to 3.0 MPa) in the gas phase (dark gray) and in the liquid phase, consisting of ammonia and dinitrile in a 2:1 ratio at a temperature of $T = 363$ K and a stirring speed of 30 s^{-1} (black) and 6.7 s^{-1} (light gray).

in intensity upon raising the stirring speed from 2.5 to 30 s^{-1} (Figure 4). At a stirring speed of 6.7 s^{-1}, the deviation from the maximum intensity was 2%. Obviously, a minimum stirring speed was required for a constant reading. Probably diffusion limitations across the stagnant liquid−solid interphase at the surface of the polymer membrane were minimized when the liquid passes the probe with a sufficiently high speed. Gas bubbles hitting the probe or gas bubbles adhering to the polymer surface cannot explain this effect, as was shown in a parallel study.[5]

The response of the signal to a pressure step in hydrogen was recorded for the gas phase and for a typical reaction mixture (at different stirring speeds). About 15 min were required in all cases until a stable reading for the MIN-100 permeation probe was observed (Figure 5). The ($t_{10} - t_{90}$) time was ∼12 min. The dead time was 0.65 min. The response time in the gas phase reflects the actual response characteristics of the instrument. The comparison of the equilibration time in the liquid phase to that in the gas phase showed that the liquid surrounding the probe has no influence on the response time. Considering the relatively slow response behavior of the probe, applications for transient measurements will be limited to slow processes. However, the major advantage of the permeation probe is that the saturation level of hydrogen in the liquid phase can be determined in situ. The second available permeation probe STD-100 showed a shorter ($t_{10} - t_{90}$) time (∼3−4 min), but it could not be used in the laboratory reactor because of its larger size. For both probes, there is a wide field of applications in process control. Note that the probe has high-temperature sensitivity with an exponential increase of permeability with temperature, as shown in a parallel study.[5]

3.2. Case Study: Hydrogenation of Dinitriles. 3.2.1. Reaction without External Mass Transfer Limitation. As a case study, the hydrogenation of an aliphatic dinitrile to diamine over a silica-supported cobalt catalyst was chosen. On an industrial scale, the reaction is frequently carried out in the liquid phase over Raney-type or supported transition metal catalysts.[9] Undesired byproducts (secondary and tertiary amines and cyclization products) are generated by intermolecular or intramolecular condensation reactions.[10] For nickel and cobalt catalysts, the presence of ammonia significantly enhances the selectivity to primary amines.[11] Liquid ammonia is, therefore, often used as a solvent in industrial processes. For high selectivities to the primary diamine, a high rate of hydrogenation (relative to the rate of condensation reactions) is essential, necessitating sufficiently high concentrations of hydrogen in the reaction mixture. Note that the overall reaction rate in such three-phase systems may be restricted by limited transport of hydrogen across the G−L or the L−S phase boundary.

3.2.1.a. Reaction Profile and Kinetics. A typical concentration profile for dinitrile hydrogenation in liquid ammonia is shown in Figure 6. One of the nitrile groups was hydrogenated first, providing aminonitrile. In a consecutive reaction, the aminonitrile was reduced to the diamine (eq 3 , X = alkyl chain). The maximum

$$\mathrm{N{\equiv}C{-}X{-}C{\equiv}N} \xrightarrow{+2H_2} \mathrm{N{\equiv}C{-}X{-}CH_2{-}NH_2} \xrightarrow{+2H_2} \mathrm{H_2N{-}CH_2{-}X{-}CH_2{-}NH_2} \quad (3)$$

concentration of the aminonitrile was relatively high (∼45% of the initial concentration of dinitrile). Simulation of the reaction sequence A → B → C based on first order reactions indicated that the first nitrile group was reduced faster than the second. However, the concentration profile was not fully consistent with this simple model. Closer inspection of the time−concentration profile showed that the concentration of the aminonitrile increased until the conversion of the dinitrile had reached ∼80% (after 30 min). At longer reaction times, the concentration of the aminonitrile decreased rapidly, which is reflected by an increased rate of diamine formation. Such a concentration profile can be explained by a stronger adsorption of the dinitrile on the catalyst surface compared to that of the aminonitrile.[12] The reaction was finished after 70 min, and almost 100% selectivity to diamine was obtained.

The concentration profile for the liquid phase is related to the integral hydrogen consumption and the hydrogen flow rate in Figure 6. The hydrogen uptake was fastest at the start of the reaction and then decreased gradually during the reaction, indicating a decrease in the overall rate of reaction. This is consistent with zero order in nitrile at high nitrile concentrations and first order in nitrile at low nitrile concentrations (see ref 6). The aminonitrile was reduced more slowly (at reaction times >30 min) than the dinitrile (after a short induction period of ∼6 min). To determine the reaction order in hydrogen, the reaction was repeated at different hydrogen pressures (Figure 7). From the initial rate of dinitrile consumption, an apparent reaction order of 0.5 in hydrogen was calculated. This is consistent with a Langmuir−Hinshelwood mechanism, similar to that suggested by Joly-Vuillemin et al. for Raney Nickel catalysts.[13]

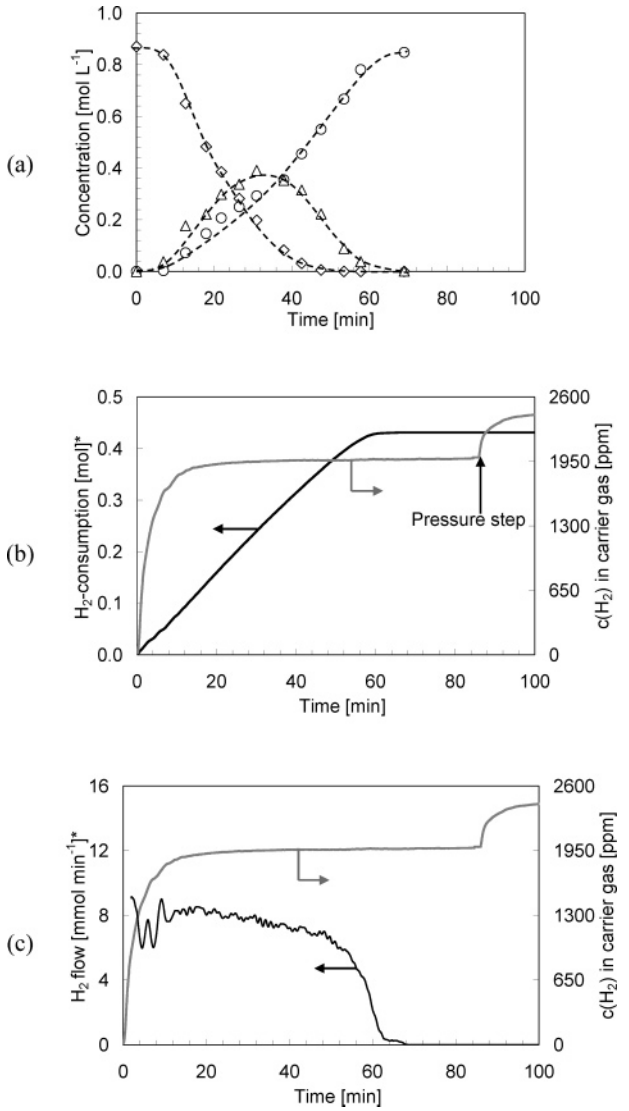

Figure 6. (a) Concentration profile of dinitrile hydrogenation at $T = 363$ K, $P_{H_2} = 3.0$ MPa, and stirring speed $N = 30$ s^{-1}: (◇) dinitrile, (△) aminonitrile, and (○) diamine. (b) Hydrogen consumption during the experiment and concentration of hydrogen in the carrier gas of the MIN-100 permeation probe (* for 112 mL solution). The arrow indicates a pressure step from 8.20 to 8.83 MPa. (c) Hydrogen flow profile and concentration of hydrogen in the carrier gas of the MIN-100 permeation probe.

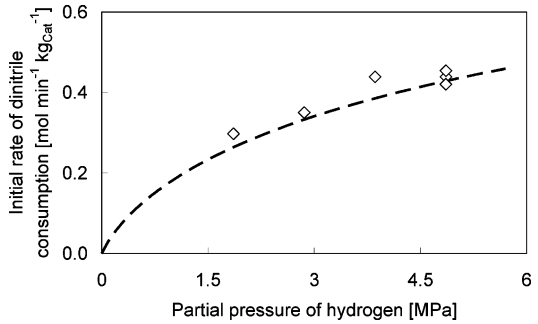

Figure 7. Initial rate of dinitrile conversion as a function of hydrogen pressure at $T = 353$ K. The line represents a Langmuir–Hinshelwood model.

3.2.1.b. Mass Transfer and Hydrogen Saturation during the Reaction. The concentration profile for the hydrogenation of the dinitrile was also related with the signal of the permeation probe (Figure 6). The hydrogen concentration in the carrier gas increased immediately after the start of the reaction to reach a constant value at 1920 ppm after ca. 15–20 min. Comparison with the progression of the signal intensity in the absence of catalyst (see Figure 5) shows that the time delay of 15 min can mostly be attributed to the equilibration time of the permeation probe. However, it can be concluded that the liquid phase was fully saturated during the final part of the reaction, as there was no change of the liquid-phase hydrogen concentration after the end of the reaction after 70 min.

The significance of mass transfer limitations during the initial phase of the reaction can also be judged from the characteristic times of reaction and mass transfer.[6] The characteristic time for the reaction was calculated from the initial rate of hydrogen uptake (1.07 mol $m_{reaction\ mixture}^{-3}$ s^{-1} at $T = 363$ K and $P_{H_2} = 3.0$ MPa) and the hydrogen concentration in the reaction mixture (93 mol m^{-3}) to 93/1.07 = 87 s. For the gas–liquid mass transfer, the characteristic time was calculated to be 0.9 s as the reciprocal value of k_La (1.1 s^{-1} at stirring speed $N = 30$ s^{-1}). The long characteristic time for the reaction compared to the gas–liquid mass transfer strongly suggests that transport of hydrogen from the gas to the liquid phase was not rate limiting. This conclusion is supported by the apparent activation energy (74 kJ mol^{-1} in the temperature range 338–388 K) which was much higher than that typically observed in the presence of external mass transfer limitations (5–10 kJ mol^{-1}).[14] The activation energy observed here was similar to that reported previously for the hydrogenation of nitriles over cobalt catalysts.[11]

3.2.1.c. Calibration and Response Behavior of the Permeation Probe. A pressure step after the end of the reaction was applied in order to calibrate the hydrogen sensor of the Fugatron and to obtain insight into the response behavior of the permeation probe upon a change of the hydrogen saturation level of the liquid. The concentration of hydrogen in the carrier gas of the permeation probe is a linear function of the partial pressure of dissolved hydrogen (P_{H_2}) in the reactor.[5] Here, the concentration of hydrogen in the carrier gas was 1992 ppm prior to the pressure step. A pressure step in hydrogen of 0.63 MPa led to an increase in the sensor signal by 428 ppm. The saturation level of 1992 ppm corresponds—according to the linear correlation P_{H_2} = (0.63 MPa × 1992 ppm)/428 ppm—to a partial pressure of hydrogen $P_{H_2} = 2.90$ MPa. This value is close to the partial pressure of hydrogen in the gas phase (3.0 MPa), which was calculated from the total pressure in the autoclave and the partial pressures of ammonia (5.12 MPa[15]) and substrate (<0.1 MPa) assuming that hydrogen behaves as an ideal dilute solution. Note that the partial pressure of dissolved gases can be derived with the permeation probe even when the system does not behave as an ideal dilute solution or when the vapor pressure is not available for each single component in the reaction mixture.

When the Henry coefficient is known, the partial pressure can be related to the concentration of hydrogen in the liquid phase according to $x_{H_2} = P_{H_2}/K_H$. However, in the case of this study, only the solubility of hydrogen in pure ammonia was reported ($\alpha = 158$ mol m^{-3} at $T = 373$ K).[16] The Henry coefficient for the reaction mixture was estimated using the initial and final pressure readings during the measurement of the k_La value for calculating the hydrogen mass balance.[17] At the conditions of the experiments shown in Figure 7,

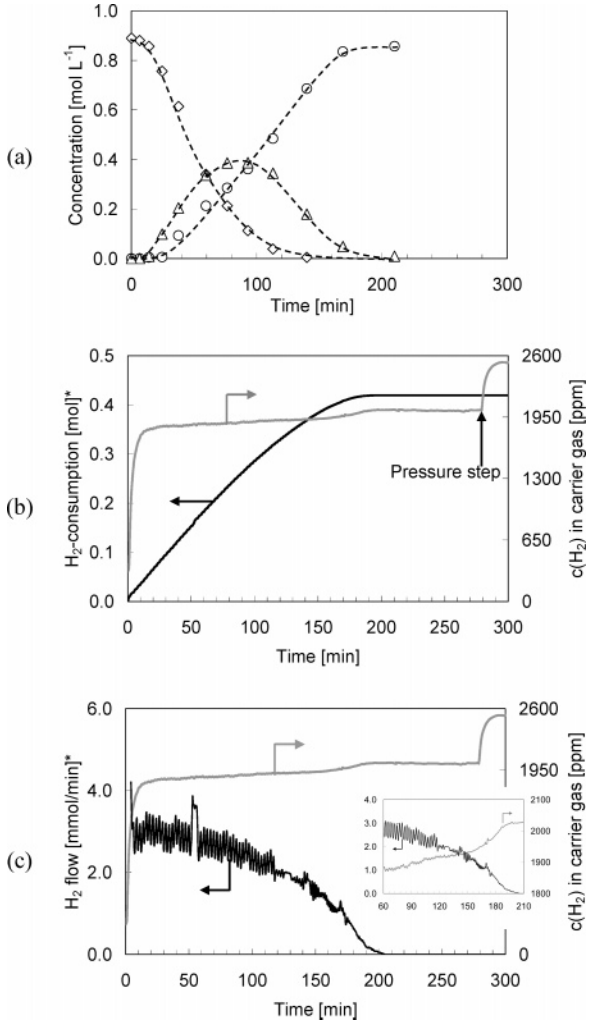

Figure 8. (a) Concentration profile of dinitrile hydrogenation at $T = 363$ K, $P_{H_2} = 3.0$ MPa, and stirring speed $N = 6.7$ s^{-1}: (◇) dinitrile, (△) aminonitrile, and (○) diamine. (b) Hydrogen consumption during the experiment and concentration of hydrogen in the carrier gas of the MIN-100 permeation probe (* for 112 mL solution). The arrow indicates a pressure step from 8.26 to 8.98 MPa. (c) Hydrogen flow profile and concentration of hydrogen in the carrier gas of the MIN-100 permeation probe. Enlarged section is shown in the inset.

the Henry coefficient was calculated to be 840 MPa and, with this value, the concentration of hydrogen in the reaction mixture was calculated to be 93 mol m^{-3} (at 3.0 MPa).

The signal intensity increased immediately after the pressure step with a steep ascent in the beginning, resulting in a relative signal increase of 50% of the final reading after 1.2 min. After 7.2 min, 90% of the final signal intensity was obtained. This shows that the hydrogen saturation level of the liquid can be followed at least qualitatively on a relatively short time scale.

3.2.2. Reaction with External Mass Transfer Limitation. An experiment at the same conditions as above but with a lower stirring speed (6.7 s^{-1}) was conducted in order to show the influence of external mass transfer (G−L or L−S) on the reaction rate and the hydrogen saturation of the liquid phase (Figure 8). Comparing the concentration profiles and the course of hydrogen uptake in Figure 8 to those in Figure 6, one can see that it takes much longer (210 min) until the end of the reaction is reached. The initial rate of dinitrile consumption (after the induction period of 6 min) is strongly reduced by external mass transfer limitations from 1.00 mol min^{-1} kg$_{cat}^{-1}$ ($N = 30$ s^{-1}) to 0.34 mol min^{-1} kg$_{cat}^{-1}$ ($N = 6.7$ s^{-1}).

The profile of hydrogen saturation of the liquid phase is related to the hydrogen consumption and to the hydrogen flow in Figure 8. Because of the response time of the MIN-100 permeation probe, only statements concerning the hydrogen saturation level of the liquid phase after the 15 min reaction time can be made. During the course of the reaction, a gradual increase in signal intensity of the permeation probe was observed. The increasing hydrogen saturation level nicely corresponds with the decreasing rate of reaction, as depicted by the hydrogen consumption profile and, even more clearly, by the hydrogen flow rate. A more detailed comparison of the hydrogen flow and the hydrogen concentration in the carrier gas is given in the enlarged section of Figure 8c to show correlations at the end of the reaction. It can be observed that the hydrogen flow and, thus, the reaction rate decreased more rapidly toward the end of the reaction (especially pronounced after 150 min). In parallel, the hydrogen saturation level increased quickly until it reached a constant value at the end of the reaction, corresponding to saturation of the liquid phase with hydrogen.

By comparing the hydrogen concentration in the carrier gas, when a reliable reading was obtained after 20 min (1830 ppm) and at the end of the reaction (2025 ppm), when the liquid is fully saturated, a relative increase in the saturation level of 10% was derived. This means that the mass transfer across the gas−liquid interface is too slow to fully replenish the hydrogen in the liquid phase during the reaction. According to Figure 7, the reaction rate depends on the hydrogen pressure—which correlates linearly with the concentration in the liquid-phase according to Henry's law—with an order of 0.5.

The observed decrease in reaction rate by almost a factor of 3 might be explained by a decrease in hydrogen concentration by a factor of 9. In this case, the hydrogen saturation level should be much lower during the reaction (∼11%) than was observed (∼90%). The explanation for this effect is that, by reducing the stirring speed, not only the G−L mass transfer rate but also the L−S mass transfer rate, across the stagnant layer surrounding the catalyst particle, is lowered. At the stirring speed investigated, the rate of the two transport steps is comparable, with the G−L mass transfer being the slower process. Thus, the liquid phase is not fully saturated during the reaction but is on a higher saturation level than expected in the absence of L−S mass transfer limitations.

Further, the characteristic times for the reaction and G−L mass transfer are compared. The characteristic time for the reaction without an external mass transfer limitation was calculated above to be 87 s. The reciprocal of the k_La value at a stirring speed of $N = 6.7$ s^{-1} (0.038 s^{-1}) is 26 s and was taken as the characteristic time for the G−L mass transfer. Thus, the characteristic time for the two processes is in the same order of magnitude. The method of characteristic times allows only for a quick estimation for the presence of G−L mass transfer limitations. In this case, this method may not allow a definitive statement about the prevailing regime.

4. Conclusions

The purpose of this study was to evaluate the potential of a new permeation probe, Fugatron by DMP Ltd., for quantifying the concentration of dissolved gases in typical three-phase reaction systems. The model reaction, cobalt-catalyzed hydrogenation of a dinitrile to diamine, was performed in a laboratory-scale slurry reactor in the presence of liquid ammonia. It is noteworthy that the reaction proceeded stepwise with the two nitrile groups of one molecule hydrogenated in two distinct steps. The observed concentration profile is consistent with stronger adsorption of the dinitrile on the catalyst surface compared to that of the aminonitrile. In consequence, the rate of aminonitrile hydrogenation increased when the dinitrile had almost depleted.

The concentration of dissolved hydrogen during the reaction was measured with the permeation probe for two regimes: one limited and one not limited by external mass transfer. The response time of the probe (12 min $t_{10}-t_{90}$) was too long to track the hydrogen concentration during the initial phase of the reaction. However, estimation of the characteristic time of the G−L mass transfer and the reaction showed that, at a stirring speed of $N = 30\ s^{-1}$, the reaction is not limited by the G−L transport step. Additionally, the activation energy (74 kJ mol^{-1}) strongly supports the assumption that L−S mass transfer limitations were absent. A steady reading of the permeation probe after 15−20 min clearly proved that the reaction mixture was saturated with hydrogen at longer reaction times.

In a second experiment, it was shown that the rate of reaction decreased significantly when lowering the stirring speed ($N = 6.7\ s^{-1}$). In this case, the signal of the permeation probe provided evidence about the saturation level as the rate of reaction was rather constant throughout the reaction. In consequence, limitations by external mass transfer were not limited to the initial phase of the reaction. The signal of the permeation probe increased during the course of the reaction in parallel with the decreasing hydrogenation rate, which is especially pronounced at the end of the reaction. Comparing the saturation level with the decrease in the hydrogenation rate upon lowering the stirring speed allowed for differentiation between G−L and L−S mass transfer, proving that G−L mass transfer was the rate-determining step. After internal calibration by a simple pressure step, the permeation probe enabled us to determine the partial pressure of dissolved hydrogen and, after determining the Henry coefficient, the concentration of dissolved hydrogen in the reaction mixture. The latter represents an interesting approach for the development of kinetic models in combination with a description of G−L mass transfer.

Acknowledgment

Xaver Hecht is thanked for experimental support. Marko Stapf is thanked for experimental assistance. Fugatron is a registered trademark of DMP Ltd.

Abbreviations

c = concentration, mol L^{-1}
K_H = Henry coefficient, MPa
k_La = volumetric gas−liquid mass transfer coefficient, s^{-1}
N = stirring speed, s^{-1}
P = pressure, MPa
P_0 = equilibrium pressure, MPa
P_{H_2} = partial pressure of hydrogen, MPa
P_f = pressure after the reaction, MPa
P_m = pressure at $t = 0$, MPa
P_{tot} = total pressure, MPa
r_0 = initial rate of reaction, mol min^{-1} kg_{cat}^{-1}
T = temperature, K
t = time, s
x_{H_2} = mole fraction of hydrogen in the liquid phase

Literature Cited

(1) Berger, R. J.; Stitt, E. H.; Marin, G. B.; Kapteijn, F.; Moulijn, J. A. Chemical reaction kinetics in practice. *CATTECH* **2001**, *5*, 30.

(2) Kapteijn, F.; Moulijn J. A. Laboratory Reactors. In *Handbook of heterogeneous catalysis*; Ertl, G., Knözinger, H., Weitkamp, J., Eds.; VCH Verlagsgesellschaft mbH: Weinheim, Germany, 1997; Vol. III, p 1359.

(3) Fugatron, DMP Ltd., www.fugatron.com (accessed Sept 2004).

(4) Dietrich, E.; Mathieu, C.; Delmas, H.; Jenck, J. Raney-Nickel catalyzed hydrogenations: Gas−liquid mass transfer in gas-induced stirred slurry reactors. *Chem. Eng. Sci.* **1992**, *47*, 3597.

(5) Meyberg, M.; Roessler, F. In-situ Measurement of Steady-State Hydrogen Concentrations during a Hydrogenation Reaction in a Gas-Inducing Stirred Slurry Reactor. *Ind. Eng. Chem. Res*. **2005**, *44*, 9705−9711.

(6) Hoffer, B. W.; Schoenmakers, P. H. J.; Mooijman, P. R. M.; Hamminga, G. M.; Berger, R. J.; van Langefeld, A. D.; Moulijn, J. A. Mass transfer and kinetics of the three-phase hydrogenation of a dinitrile over a Raney-type nickel catalyst. *Chem. Eng. Sci.* **2004**, *59*, 259.

(7) Lekhal, A.; Chaudhari, R. V.; Wilhelm, A. M.; Delmas, H. Gas−liquid mass transfer in gas−liquid−liquid dispersions. *Chem. Eng. Sci.* **1997**, *52*, 4069.

(8) *User Manual Fugatron HYD-200*; DMP Ltd.: Switzerland, 2004.

(9) Huang, Y.; Adeeva, V.; Sachtler, W. M. H. Stability of supported transition metal catalysts in the hydrogenation of nitriles. *Appl. Catal., A.* **2000**, *196*, 73.

(10) Mares, F.; Galle, J. E.; Diamond, S. E.; Regina, F. J. Preparation and characterization of a novel catalyst for the hydrogenation of dinitriles to aminonitriles. *J. Catal.* **1988**, *112*, 145.

(11) Volf, J.; Pasek, J. Hydrogenation of nitriles. In *Studies in surface science and catalysis*; Cerveny, L., Ed.; Elsevier: Amsterdam, The Netherlands, 1986; Vol. 27, p 105.

(12) For similar conclusions on Raney Nickel catalysts, see Joucla, M.; Marion, P.; Grenouillet, P.; Jenck, J. Comparative catalytic hydrogenation reactions of aliphatic dinitriles over Raney Nickel catalysts. In *Catalysis of organic reactions III*; Kosak, J. R., Johnson, T. A., Ed.; Marcel Dekker: New York, 1994; p 127.

(13) Joly-Vuillemin, C.; Gavroy, D.; Cordier, G.; De Bellefon, C.; Delmas, H. Three-phase hydrogenation of adiponitrile catalyzed by Raney Nickel: Kinetic model discrimination and parameter optimization. *Chem. Eng. Sci.* **1994**, *49*, 4839.

(14) Emig, G.; Dittmeyer, R. Simultaneous heat and mass transfer and chemical reaction. In *Handbook of heterogeneous catalysis*; Ertl, G., Knözinger, H., Weitkamp, J., Eds.; VCH Verlagsgesellschaft mbH: Weinheim, Germany, 1997; Vol. III, p 1359.

(15) Lemmon, E. W.; McLinden M. O.; Friend, D. G. Thermophysical Properties of Fluid Systems. In *NIST Chemistry WebBook*; Linstrom, P. J., Mallard, W. G., Eds.; NIST Standard Reference Database Number 69; National Institute of Standards and Technology: Gaithersburg, MD, 2003; p 20899; http://webbook.nist.gov.

(16) Stephen, H.; Stephen, T. *Solubilities of inorganic and organic compounds.* Pergamon Press: Oxford, U.K., 1963; Vol. 1.

(17) Purwanto; Desphande, R. M.; Chaudhari, R. M.; Delmas, H. Solubility of hydrogen, carbon monoxide, and 1-octene in various solvents and solvent mixtures. *J. Chem. Eng. Data* **1996**, *41*, 1414.

Received for review May 23, 2005
Revised manuscript received September 8, 2005
Accepted September 8, 2005

IE050612Y